Sensors & Actuators: B. Chemical 286 (2019) 306–314

Contents lists available at ScienceDirect

Sensors and Actuators B: Chemical

journal homepage: www.elsevier.com/locate/snb

Simultaneous *in situ* temperature and relative humidity monitoring in mechanical ventilators using an array of functionalised optical fibre long period grating sensors

Jiri Hromadka[a,b], Nurul N. Mohd Hazlan[a], Francisco U. Hernandez[a], Ricardo Correia[a], A. Norris[c], Stephen P Morgan[a], Sergiy Korposh[a,*]

[a] Optics and Photonics Group, Faculty of Engineering, University of Nottingham, University Park, Nottingham NG7 2RD, UK
[b] Institute for Environmental Studies, Faculty of Sciences, Charles University in Prague, Benátská 2, CZ 12843 Praha 2, Czech Republic
[c] Queens Medical Centre, Nottingham University Hospital Trust, Nottingham, UK

ARTICLE INFO

Keywords:
Optical fibre sensor
Long period grating (LPG)
Healthcare monitoring
Endotracheal tube
Multiplexing
Temperature
Relative humidity (RH)
Mechanical ventilation

ABSTRACT

An array of optical fibre long period gratings (LPGs) has been demonstrated for biomedical application to monitor temperature and relative humidity (RH) changes in the air delivered by a mechanical ventilator operating in different modes. The LPG array consists of two gratings, where one was kept bare to monitor the temperature change and the second was modified with 10 layers of silica nanoparticles to measure relative humidity.

A mesoporous film was deposited on the surface of an optical fibre LPG using the layer-by-layer method. The sensor was calibrated in a bench model against a commercially available temperature and relative humidity sensor and sensitivity of the sensor was 0.46 ± 0.01 nm/ °C and 0.53 nm/RH%, respectively.

The tip of the sensor array was modified with reflection mirror and placed inside an endotracheal tube (ETT) and tested in typical clinical equipment to enable the in-situ real-time monitoring of humidity and temperature. Temperature and RH changes associated with the breathing frequency of 8 and 15 breaths per minute were successfully monitored using developed sensor array.

1. Introduction

Artificial ventilation via a tracheal tube is integral to critical care and anaesthesia [1]. Over 1 million endotracheal tubes (ETT) are placed in patients' tracheas annually in the UK to support artificial ventilation and/or protect the lungs from inhalation of blood or gastric contents. At any time, around 2000 patients on Intensive Care Units (ICUs) in the UK are receiving artificial ventilation via ETTs, and annually around 20,000 patients require these devices in Emergency Departments [2]. Though crucial to maintain life in the above situations, the presence of such devices is associated with very significant problems such as risk of ventilated associated pneumonia (VAP), drying of the mucosal layer and development of post-intubation tracheal stenosis (PITS) [3].

Gas conditioning, and specifically appropriate warming and humidification, is an important aspect of respiratory care in patients where normal nasal and oral passages have been bypassed by an ETT [4]. Maintenance of respiratory function of mechanically ventilated patients requires adequate humidification. Inadequate warming and humidification of inspired gases has been associated with functional deterioration of nasal mucosa. In addition, there is a correlation between humidification and ventilated associated pneumonia (VAP) risk. Higher levels of humidity to the airway (44 mg water vapour/l gas) can facilitate maximal mucociliary clearance and hence reduce the risk of biofilm formation. VAP is the device centred infection responsible for the largest number of deaths, around 100 K, and for €5.2bn hospital costs in Europe per annum [5].

One of the challenges to overcome in humidification is to monitor the humidity level as close to the patient's lungs as possible. In current clinical practice, humidity and temperature of the delivered artificial air is monitored in the breathing tubing some distance from the patient, which due to cooling effects doesn't provide adequate information on the humidity and temperature of the air delivered into lungs [2].

The air delivered during mechanical ventilation into the airways of intensive care patients is usually humidified using a heated water bath. A heating element runs down the gas delivery tubing to the patient to

* Corresponding author.
E-mail address: s.korposh@nottingham.ac.uk (S. Korposh).

https://doi.org/10.1016/j.snb.2019.01.124
Received 29 June 2018; Received in revised form 7 January 2019; Accepted 25 January 2019
Available online 28 January 2019
0925-4005/ © 2019 The Authors. Published by Elsevier B.V. This is an open access article under the CC BY license (http://creativecommons.org/licenses/BY/4.0/).

maintain gas temperature and prevent condensation. Temperature and humidity sensors at the end of the breathing circuit are linked to servo-controlled systems to adjust the output of the water bath to maintain temperature and humidity at the distal (patient) end of the circuit. However, the sensors at the end of the circuit are still external. Current sensors are not capable of performing humidity measurements in-situ, directly inside the endo-tracheal tube [6]. The development of new in-vivo sensors is in high demand.

The inclusion of a monitoring system within the ETT will enable clinicians to monitor more closely the condition of gases and the ETT environment to protect against development of VAP and allow intervention at an earlier stage, potentially preventing the causes of VAP, personalizing treatment, and increasing the quality of healthcare.

Sensing techniques based upon optical fibre devices can be used to probe the optical characteristics of materials that exhibit changes in their optical properties upon exposure to targeted chemical species [7–9]. Such devices are particularly attractive in light of their high sensitivity, selectivity, the ready ability to multiplex arrays of sensors and the prospect for remote sensing. In addition, silica optical fibres are biocompatible, which allows them to be used within the human body, and allows effective operation in gaseous and liquid media, making it a universal platform for sensor development.

Along with the optical fibre, biocompatibility of the materials used for the fabrication of the sensitive film is equally important. In this work, the sensitive layer was formed using an electrostatic self-assembly layer-by-layer approach using poly(allylamine hydrochloride), PAH, and SiO_2 NPs. Biocompatibility of PAH was previously examined *in vitro* using haemobiocompatibility studies, cytotoxicity and comet assay in peripheral blood mononuclear cells [10]. It was demonstrated that PAH nanocapsules are biocompatible and non-toxic, thus suggesting their potential for *in vivo* applications [10]. Although there have been a number of reports conducted on toxicity and biocompatibility of SiO_2 NPs their conclusions have been very different, making it difficult to link physicochemical properties of SiO_2 NPs types to toxicity, bioavailability, or human health effects [11]. In all reports, the toxicity of SiO_2 NPs is generally concentration dependent and at lower concentrations SiO_2 NPs can be regarded as biocompatible [12]. In this work the amount of the SiO_2 NPs (0.5 mg) deposited onto the surface of the optical fibre sensors is below the toxicity threshold level, and SiO_2 NPs are embedded into the robust film, which decreases the chance of penetration into the human body, which we consider makes the developed sensors biocompatible.

Fibre-optic sensing platforms are small, lightweight, immune to electromagnetic interference and as such can be used in extreme conditions, enabling remote real time monitoring with no electrical power needed at the sensing point [13]. This offers an attractive practical solution to conduct in situ measurements in the ICU.

Among the different types of fibre-optic sensors, those based on gratings, specifically LPGs, have been employed extensively for refractive index measurements [14] and for monitoring associated chemical processes [7,15], since they offer wavelength-encoded information, which overcomes the referencing issues associated with intensity based approaches.

An LPG consists of a periodic perturbation of the refractive index of the fibre core, which couples the core mode to the co-propagating cladding modes of the fibre. This coupling is manifested in the transmission spectrum of the optical fibre as a series of resonance bands. Each resonance band corresponds to coupling to a different cladding mode and thus shows different sensitivity to environmental changes [16].

The coupling wavelength can be obtained from the following phase matching equation

$$\lambda_x = (n_{core} - n_{clad(x)})\Lambda \quad (1)$$

Where λ_x represents the wavelength at which light is coupled to the LP_{0x} cladding mode, n_{core} is the effective refractive index of the mode propagating in the core of the fibre, $n_{clad(x)}$ is the effective index of the LP_{0x} cladding mode and Λ is the period of the LPG [16]. The central wavelength of the resonance band is sensitive to changes in the surrounding environment such as temperature or external index of refraction [16]. LP_{0x} cladding modes represent the approximation of the behaviour of the light propagating through the fibre however still provide enough accuracy to be used for the calculation and modelling of LPG properties [17].

The key element of an LPG based chemical sensor is the sensitive layer that captures the analyte. Among the various techniques used for the deposition of the sensitive element, layer-by-layer (LbL) assembly is considered highly versatile, enabling control over the structure of the deposited material. This technique can be used to deposit a wide range of materials onto a range of substrates and represents a cheap, simple and rapid approach for thin film deposition [18]. Silica nanoparticles have been proven to provide the sensitivity to RH due to the adsorption of water molecules in the mesoporous structure of the film [19], and a range of the fibre optic RH sensors using different sensing platforms and SiO_2 nanoparticles (NPs) [19,14,20]. Some other materials have been also used as functional layers in fibre optic humidity sensors, such as tungsten disulfide [21], reduced graphene oxide (rGO) [22] or zinc oxide [23]. However, SiO_2 nanoparticles thin films prepared using layer-by-layer approach offer several advantages such as high surface area and hydrophilicity, easy fabrication and control of the thickness during the deposition over other reported methods. Fibre optic relative humidity sensors have been recently reviewed in [24].

LPG multiplexing enables the simultaneous measurement of multiple parameters [14]. As the LPG is sensitive to temperature, the implementation of the LPG based chemical sensor into an LPG array represents the most effective option for any temperature measurement and thus enables multi-parameter in-situ monitoring [14]. An alternative is to use a single LPG partially coated by a sensitive film, where the signal from both parts is separated during the post processing [25].

In our previous work we have demonstrated temperature and RH monitoring of the air delivered by a mechanical ventilator using fibre optic sensors based on a fibre Bragg grating and a thin film deposited on the fibre tip creating a Fabry-Perot cavity [19]. In this paper, we propose the simultaneous measurement of temperature and RH of the air delivered by a mechanical ventilator in non-breathing (constant flow rate) and breathing (alternate flow rate, which is related to the breathing rate) modes using an LPG array. The advantages of the current method are the ability to use relatively low cost equipment and the higher sensitivity to temperature and RH of LPG sensors over their FBG counterparts.

A sensor array consisting of 2 LPGs with different grating periods of 108.8 and 109.0 μm combined in a single optical fibre was used for simultaneous measurements of temperature and relative humidity. The LPGs have periods selected such that they operate near the phase matching turning point (PMTP) and that differ by 0.5 μm to facilitate wavelength division multiplexing [26]. A mesoporous coating of silica nanospheres was deposited onto one of the LPGs, such that it was sensitive to RH. The surface of the other was left unmodified to measure temperature. The sensor was placed inside an endotracheal tube to enable the in-situ, real time measurement in mechanical ventilation.

2. Methodology

2.1. Materials

Poly(allylamine hydrochloride) PAH (Mw: 75,000), potassium hydroxide, ACS reagents and ethanol were purchased from Sigma-Aldrich. SiO_2 nanoparticles (NPs)(SNOWTEX 20 L) were purchased from Nissan Chemical. All of the chemicals were analytical grade reagents and used without further purification. Deionized water (18.3 MΩ cm) was obtained by reverse osmosis followed by ion exchange and filtration

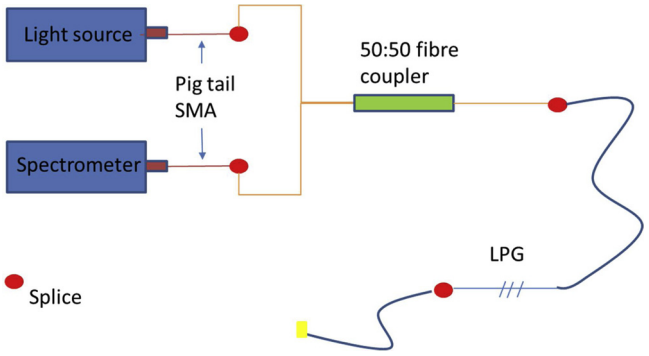

Fig. 1. Schematic illustration of the fibre optic sensing array operating in the reflection mode. Light from a halogen source is delivered to the sensing array and is reflected from the tip of the fibre, returning to a spectrometer via a 1 × 2 fibre optic coupler.

(Millipore, Direct-QTM).

2.2. Sensor design

An LPG array used for temperature and humidity sensing was operating in reflection mode and is shown in Fig. 1. The tip of the 50:50 1 × 2 single mode fibre coupler was coated with gold using sputtering technique to create a ca. 50 nm thin reflection mirror. LPG2 was coated with SiO_2 nanoparticles and further used for RH monitoring and LPG1 was kept bare to track the temperature changes. The reflection spectrum of the optical fibre was recorded by coupling the output from a tungsten-halogen lamp (Ocean Optics HL-2000) into the fibre and analysing the reflected light using a fibre coupled CCD spectrometer (Ocean Optics HR4000).

2.3. Sensor fabrication

For better grating period control and faster inscription process, two different methods were used to inscribe LPGs with different period in the core of the optical fibre. LPGs with grating periods of 108.8 (LPG1) and 109.0 µm (LPG2) and length of 30 mm were fabricated in photosensitive boron–germanium co-doped optical fibre (Fibercore PS750) by exposing the fibre to 266 nm wavelength laser light using fabrication via point by point technique for LPG1 and fabrication using an amplitude mask for LPG2, using the procedures described in [27] and [28] respectively.

There are two methods available for fabrication of LPGs: point by point scanning of a laser beam; and amplitude mask where light illuminates a mask and projects the grating structure onto the fibre. Fabrication of the LPG using a point by point technique allows better grating period control, while fabrication using an amplitude mask allows much faster fabrication time to be achieved for the same laser inscription parameters. The LPG fabrication method using amplitude masks restricts the grating period to the availability of masks, which in our case provides LPGs with a separation of 0.5 µm, which will not provide operation of one of the gratings in PMTP and sufficient wavelength separation between the attenuation bands for multiplexing in the wavelength domain. The grating period of two gratings was chosen such that attenuation bands corresponding to two different gratings could be distinguished in the transmission spectrum allowing for LPG array multiplexing in the wavelength domain [14].

The grating period was selected such that the LPGs operated at or near the phase matching turning point, which, for coupling to a particular cladding mode (in this case LP_{019}), ensured optimized sensitivity [29].

Each LPG is associated with distinct and uniquely identifiable resonance band in the spectrum, which enables multi-parameter measurements.

The LPG2 was coated with 10 layers of silica nanoparticles following the process described in the next section. Individual LPGs were spliced into a single fibre (using Fujikura 70S fusion splicer) and further spliced to the connections of the fibre coupler (50:50, 1 × 2 single mode F-CPL-S12785, Newport, UK). A gold layer of over 50 nm was sputtered on the distal end of the fibre to enable the sensors to operate in reflection mode.

2.4. Functional coating deposition

A mesoporous thin film of SiO_2 NPs was deposited onto LPG2 using an electrostatic self-assembly approach that has been described elsewhere [30]. The region of the optical fibre containing LPG2 was fixed in a Teflon holder constructed with a compartment to accommodate a solution. The optical fibre was rinsed with deionized water and immersed in a 1 wt% KOH in ethanol/water = 3:2, v/v solution for 20 min, leading to negatively charged surface. The optical fibre was then immersed sequentially into a solution containing a positively charged polymer, PAH, and a solution containing negatively charged SiO_2 NPs, for 15 min each, resulting in the alternate deposition of PAH and SiO_2 NPs layers on the surface of the fibre. The fibre was rinsed with distilled water and dried by flushing with nitrogen gas after each deposition step. A 10 cycle $(PAH/SiO_2)_{10}$ film was deposited onto LPG2.

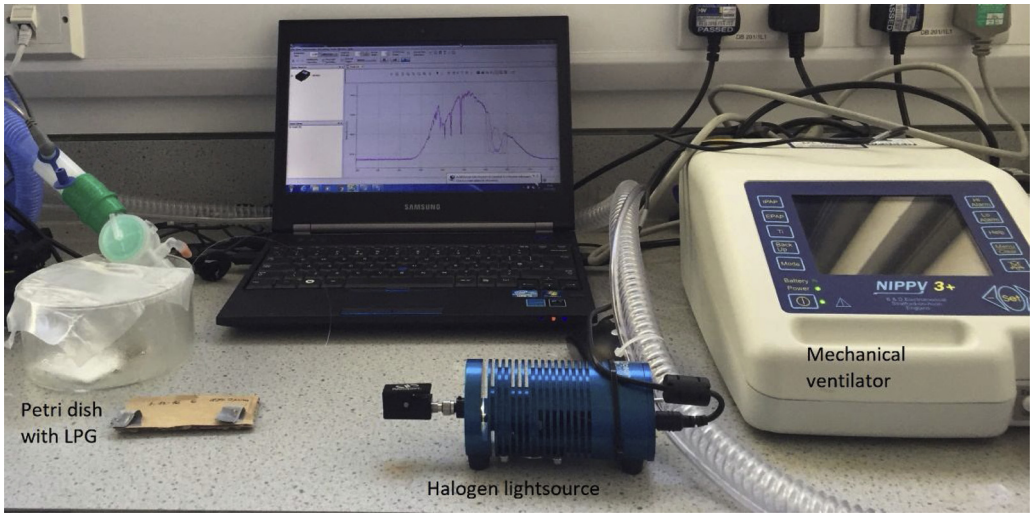

Fig. 2. Experimental setup for monitoring of temperature and RH delivered by a mechanical ventilator (the LPGs are placed inside the Petri dish).

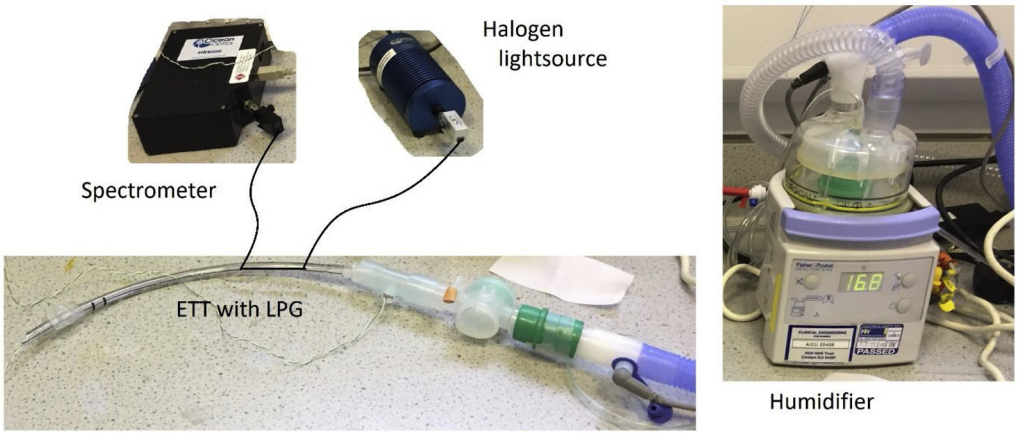

Fig. 3. Experimental set up for the experiment conducted in Petri dish.

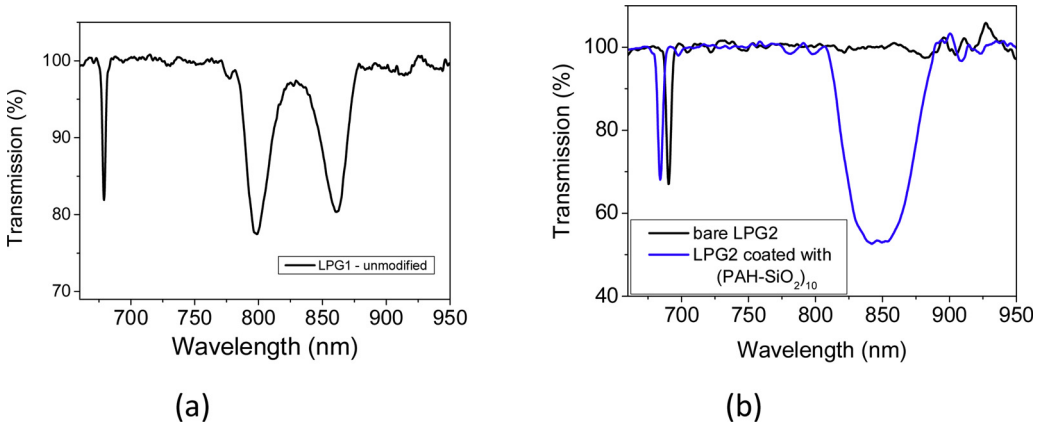

Fig. 4. Transmission spectra of a) LPG1 and b) LPG2 before (black) and after (blue) the deposition of 10 layers of PAH-SiO2 functional coating. All spectra are taken as single LPGs in transmission mode (For interpretation of the references to colour in this figure legend, the reader is referred to the web version of this article).

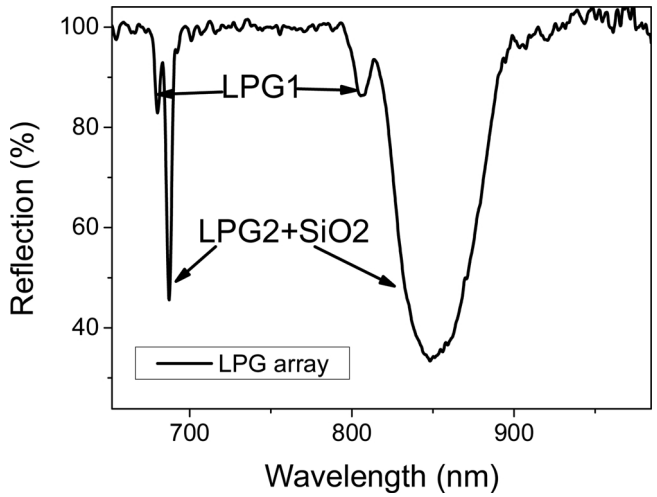

Fig. 5. Reflection spectrum of LPG array: LPG1 was kept unmodified, LPG2 was coated with 10 layers of silica nanoparticles, after the splicing and the spectrum was taken in a reflection mode.

The number of layers was chosen carefully such that the device possesses enough sensitivity to the measurand and that the resonance bands corresponding to the individual LPGs could be resolved after the deposition of the coating.

2.5. Calibration of the sensors - inside a Petri dish in flow mode

The temperature and RH responses of the LPGs were characterized over a range from 25 to 38 °C and 35–98 RH% respectively, by placing the LPGs in a Petri dish covered by a plastic film, exposed to the outlet from the mechanical ventilator (NIPPY3+, B&D Electromedical Ltd), Fig. 2. The acquisition interval was set to 500 ms.

A temperature data logger (One Wire, iButton®HygrochronTemperature/Humidity Logger, part number DS1923, from MaximIntegratedTM), with precision of ± 0.5∘C and ± 0.6 RH%, was placed inside the Petri dish in proximity to the LPGs. The central wavelengths of the attenuation bands were determined from the recorded transmission spectrum and further used for the calibration of the sensors.

2.6. Environmental testing – breath cycles

The LPG array was placed inside an endotracheal tube and exposed to air delivered by a mechanical ventilator, Fig. 3, using the same set up as described above and shown in Fig. 2.

3. Results and discussion

3.1. Fabrication and functionalisation of LPG sensor array

Fig. 4a shows the transmission spectrum of LPG1 (used for temperature measurement) in air. The attenuation band at ca. 679 nm for this grating period corresponds to the coupling of the core mode to the

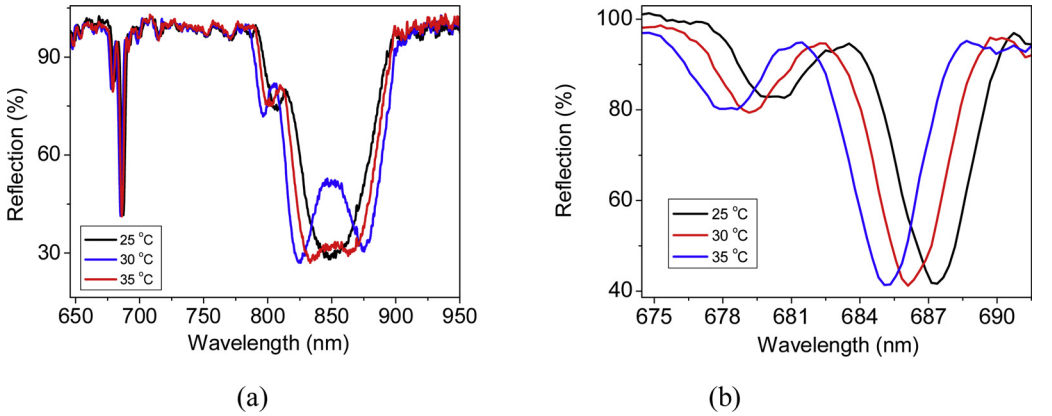

Fig. 6. (a) The response of the reflection spectrum of the sensing towards different temperature levels, the reflection spectrum taken at: black line, 25 °C; red line, 30 °C ; and blue line, 35 °C. (b) shows detailed information of LP_{018} attenuation band in the wavelength range of 675–690 nm. As expected [14] both LPGs respond to the temperature change with the highest sensitivity for both LPGs observed for LP_{019} attenuation band (For interpretation of the references to colour in this figure legend, the reader is referred to the web version of this article).

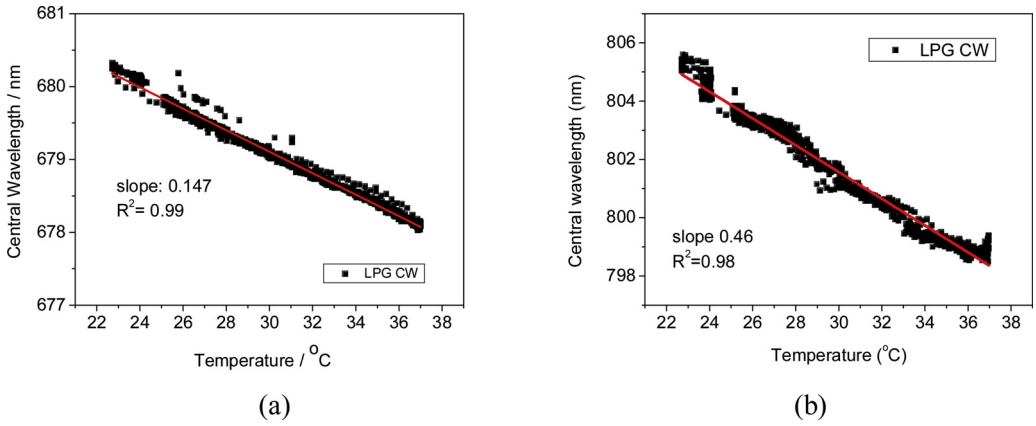

Fig. 7. Temperature calibration curve for (a), attenuation band LP_{018} and (b) attenuation band LP_{019} of unmodified LPG1; (the data were taken from all transmission spectra over two increase and decrease cycles).

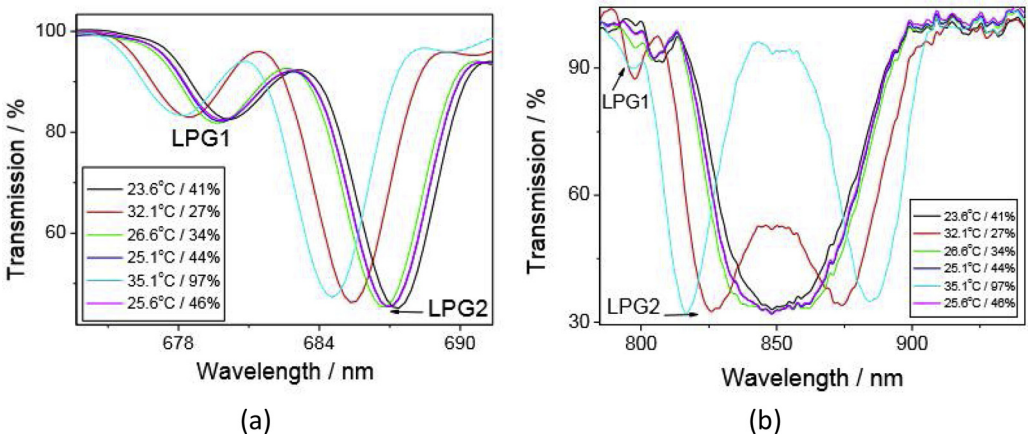

Fig. 8. Reflection spectrum of an LPG array exposed to different temperature and RH levels: (a) attenuation bands corresponding to LP_{018} and (b) LP_{019} cladding modes.

linearly polarized LP_{018} cladding mode, while two attenuation bands at ca 799 nm and 862 nm correspond to the coupling of the same LP_{019} cladding mode as LPG operates at the PMTP [30,31]. The typical sensitivity of this sensor to temperature is 0.5 nm/°C [14], which is ca 50 times higher than the typical sensitivity of FBG sensors [32].

Fig. 4b shows the transmission spectrum of LPG2 (used for RH measurements) measured in air before (black line) and after (blue line) deposition of 10 layers of SiO_2 NPs. Similar to LPG1 the attenuation band at ca. 690 nm corresponds to the LP_{018} cladding mode. However, since the grating period of LPG2 is larger than the grating period of LPG1 the attenuation band is red-shifted and also there is no coupling to the LP_{019} cladding mode. After the deposition of the SiO_2 NPs thin film the band shifts to shorter wavelengths (ca. 684 nm) due to the presence of the coating on the surface of the LPG. On the other hand, the broad attenuation band with the central wavelength at ca. 848 nm corresponding to the LP_{019} cladding mode is not split into two bands because of the higher grating period compared to LPG1 and is fully developed. This behavior is well reported in the literature [33].

The transmission spectrum of the LPG operating at the PTMP shows one broad "U" shape attenuation band, where an LPG in the proximity to the PMTP shows two discrete separate bands, but both bands correspond to the coupling to the same cladding mode. The same effect of

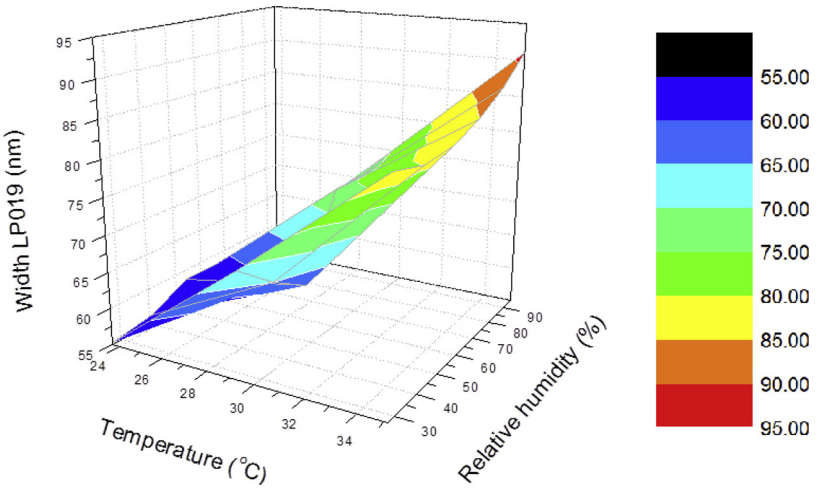

(a)

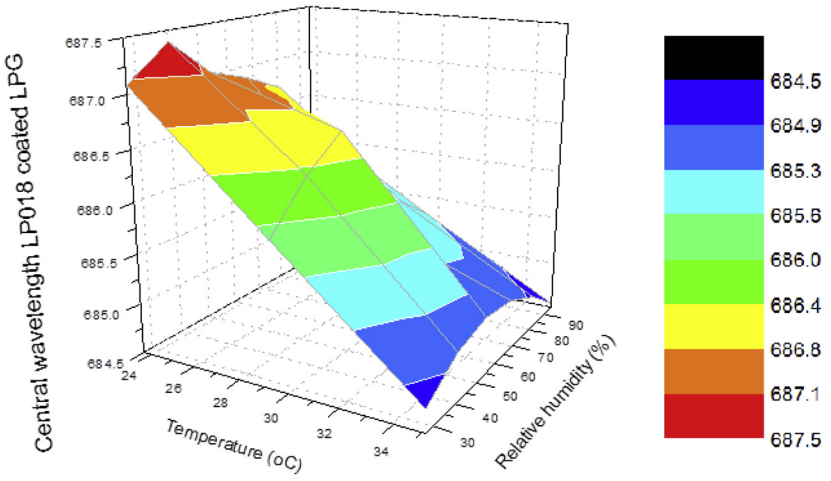

(b)

Fig. 9. The position of (a) LP_{019} of the coated LPG2 as a function of temperature and RH and (b) the central wavelength of LP_{018} of.

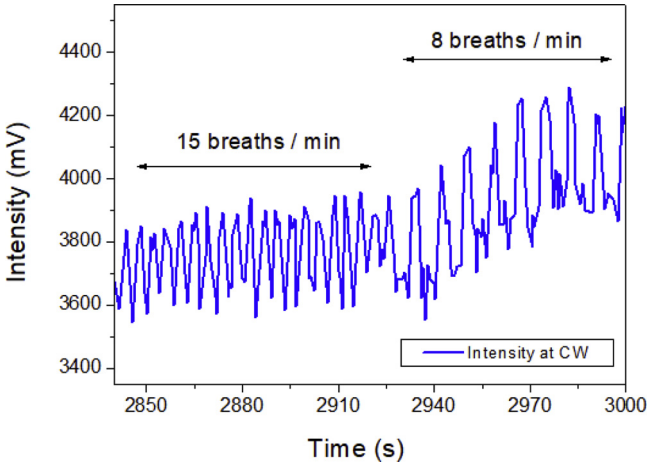

Fig. 10. The reflected intensity level at the central wavelength of LPG1 showing the sensor's response to the temperature changes associated with breathing.

the splitting of the "U" shape band into two can be observed when the LPG is exposed to temperature and RI change (increase). This behaviour follows from phase matching Eq. (1), and can be visualized using phase matching curves, described e.g. in [27].

After fabrication of the individual LPGs, they were spliced in series to the common channel of a 1 × 2 coupler (Fig. 1) and the tip of the sensor was coated with the Au thin film using sputtering. Fig. 5 shows the reflection spectrum of the LPG sensing array after splicing and after the deposition of SiO_2 nanoparticles on LPG2. As can be seen from Fig. 5 after splicing distinct attenuation bands are present for both LPG1 and LPG2 (indicated by arrows) demonstrating the feasibility of wavelength division multiplexing of the LPG array.

It should be noted, however, that the attenuation is much stronger for LPG2 as compared to LPG1 and also that the second separated peak of LPG1 is superimposed with broad U-band of LPG2 and therefore cannot be clearly distinguished. Nevertheless tracking the position of the first separated peak of LPG1 proves to be sufficient for simultaneous measurements of temperature and RH.

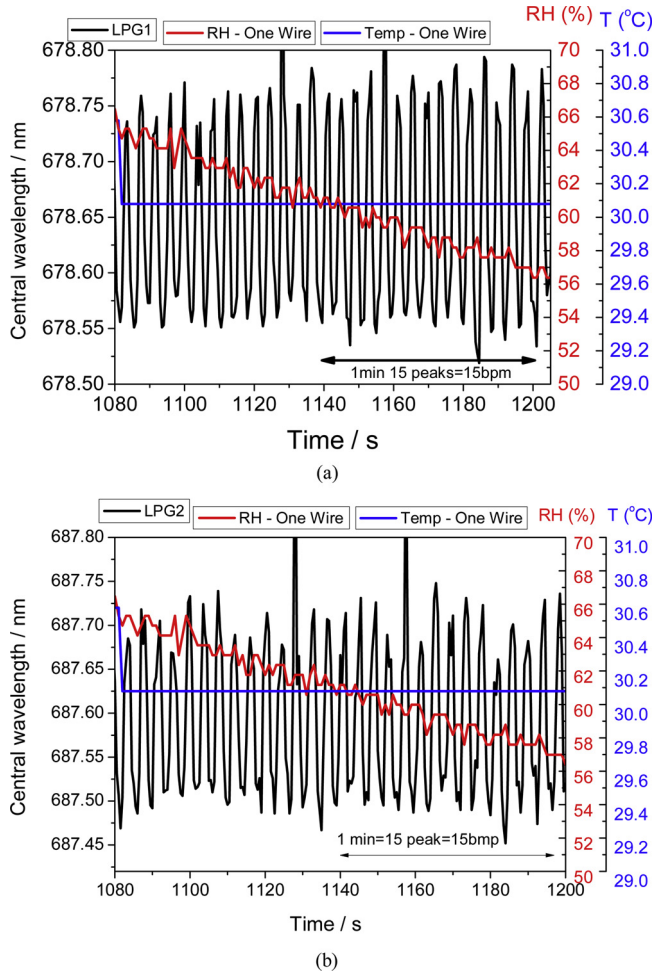

Fig. 11. Position of the central wavelength of LP_{018} of the (a), LPG1, (b), coated LPG2 (black) as a response to breath to breath change in temperature (15 bpm), there is no breath to breath response from a commercial device one wire (red and blue) (For interpretation of the references to colour in this figure legend, the reader is referred to the web version of this article).

3.2. Temperature and RH calibration

After fabrication of the LPG array it was exposed to known values of temperature and humidity using the set up shown in Fig. 2. The attenuation bands corresponding to LP_{018} for both LPG1 and LPG 2 shift to shorter wavelengths as temperature increases from 25 to 37 °C, Fig. 6. The sensitivity of this attenuation band to temperature is ca. 0.147 ± 0.01 nm/°C. The second attenuation band (LP_{019}) for the unmodified LPG1 also shifts to lower wavelengths and the sensitivity is 0.46 ± 0.01 nm/°C, while for LPG2 the band splits as the temperature increases from 25 to 37 °C, Figs. 6 and 7. It should be noted, that although RH will change with the temperature as well, bare LPGs are not sensitive to the RH changes [14].

Following the temperature calibration, the LPG array was exposed to different RH values. The LPG array responds to temperature, but only LPG2 is sensitive to RH change, as the bare LPG is not sensitive to the RH [14], Fig. 8. As can be seen in Fig. 8a when both temperature and RH were changed only relatively small wavelength shift (ca. 1 nm) was observed for the unmodified LPG1 due to the temperature change, while much larger shift of ca. 4 nm was observed for SiO_2 NPs coated LPG2 due to a RH change. This difference between LPG1 and LPG2 is more prominent when LP_{019} is considered, Fig. 8b, where the change of the LPG2 is ca. 30 nm, while 2 nm change is observed for the LPG1 attenuation band. The estimated sensitivity to RH of the coated LPG2

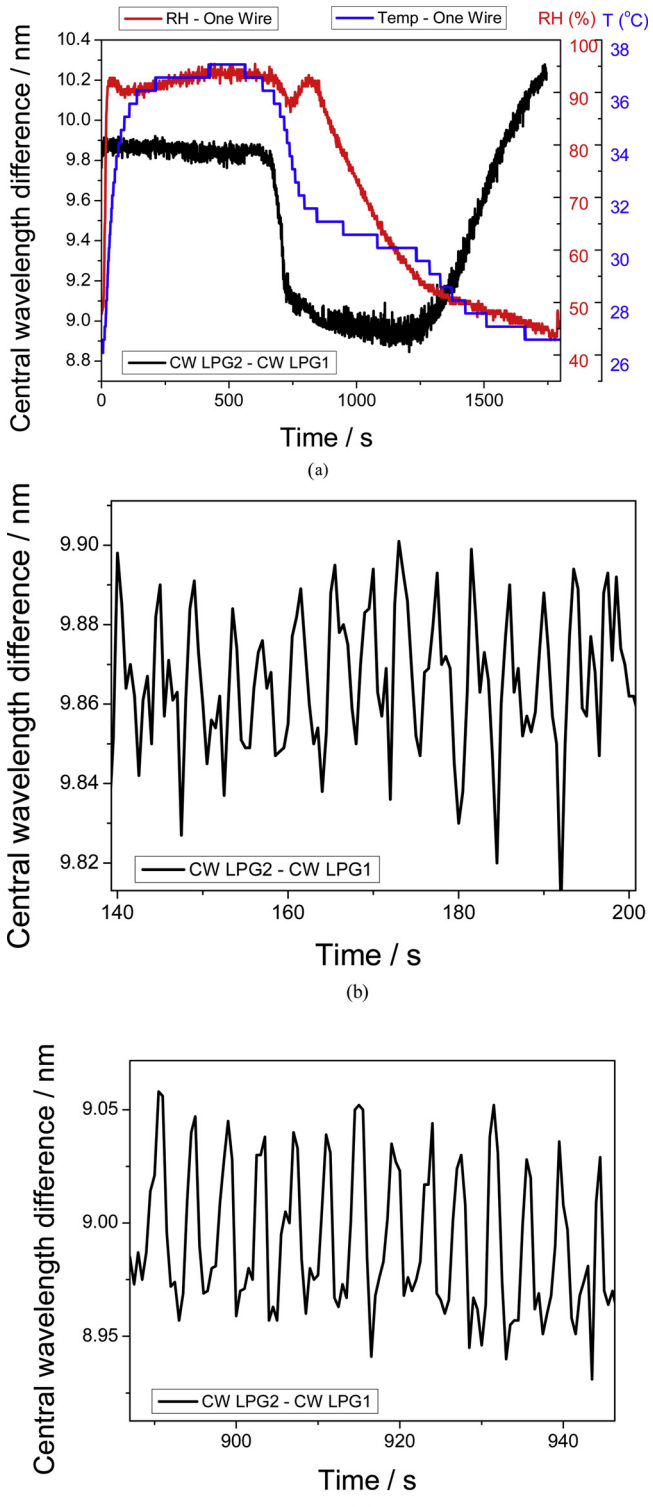

Fig. 12. a) Position of the central wavelength difference of LP_{018} of the coated LPG2-LPG1 as a response to breath to breath change in temperature (15 bpm), there is no breath to breath response from a commercial device one wire (red and blue) and the details of 1 min period (data taken from Fig. 12a) where the RH was b) ≈ 95 and c) 50 RH%.

was estimated to be 0.05 nm/RH% for LP_{018} and 0.53 nm/RH% for LP_{019}. Based on the spectrometer resolution and sensitivity of the LPG to RH and temperature even changes as small as 0.5 °C and 3% can be resolved using developed LPG sensor array.

Since the coated LPG2 is sensitive to both temperature and RH, to

determine RH values the temperature needs to be calculated using the values taken from the bare LPG1. The sensitivity of LP_{018} and LP_{019} of LPG2 towards temperature and RH is shown in Fig. 9a and b, respectively.

It should be noted that the maximum temperature observed in Fig. 9 is 1–2 °C lower than in Fig. 7. In the latter figure, results were obtained with the LPG fixed in a petri dish that is closer to the outlet of the mechanical ventilator/humidifier, while in Fig. 9 the LPG is fixed in the ETT and there is a temperature drop between the outlet of the ventilator/humidifier and this position. The core body temperature is around 37 °C and it is required that the delivered air should be close to this value. However, it should be noted that it was impossible to achieve higher than 35 °C temperature values using the mechanical ventilator typically used in ICU. This suggests that the delivered air is actually at lower than 37 °C temperature and that improvements could be made to this equipment justifying the requirement of near patient measurement. The developed sensor could allow more accurate titration of settings to achieve desired effects in the patient.

3.3. LPG sensor testing in situ

The sensor responded to the temperature and RH changes associated with the different breathing frequencies of 15 and 8 breath cycles per minute, Fig. 10. The capability of distinguishing between individual breaths indicates the high sensitivity and rapid response time of the fibre optic sensor. The small increase in the baseline when switched to 8 breath/ min is owing to the small increase in the temperature as slower breathing rate and hence flow rate is applied.

Fig. 11 shows the change in position of the central wavelength of LP_{018} for an LPG array where unmodified LPG1, Fig. 11a, shows the change to temperature, while LPG2, Fig. 11b, shows the combined change of the temperature and humidity. Subtraction of the temperature effect may be done using the difference between the positions of central wavelengths (LP_{018}) of the coated LPG2 and bare LPG1, Fig. 12.

Fig. 12a demonstrates central wavelength shift for LP_{018} associated with the humidity change. Clear patterns corresponding to the breathing rate of 15 breath per minute can be observed from the difference in the position of the central wavelength of both LPGs. Moreover, as can be seen from insets in Fig. 12b and 12c the array can track changes at both high (95% RH, inset A) and low (45% RH, inset B) levels of relative humidity.

The obtained results clearly demonstrate that fabricated LPG array can be used in mechanical ventilators to measure *in situ* variations in temperature and relative humidity. Using the calibration curve obtained in Figs. 7 and 8 the breath to breath temperature variation in mechanical ventilator can be estimated to be around 2 °C while for humidity an estimated variation is ca. 1.5%, which correlates well with reported results [34]. It was also demonstrated that the LPG sensor is more sensitive and has faster response time to temperature and humidity changes compared to commercial devices.

4. Conclusions and further work

Multiparameter monitoring of temperature and relative humidity using an LPG array has been demonstrated for monitoring of air delivered during mechanical ventilation. The LPG array presented enabled measurement of temperature and RH changes with sensitivity of 0.46 ± 0.01 nm/°C and 0.53 nm/RH%, which was related to non-breathing and breathing mode at two different respiratory rates of the mechanical ventilator typically used in clinical settings. Further work in this area will cover the optimization of the sensitivity via the change of the coating thickness and the grating period. Further functionalization of the coating of additional LPGs, e.g. towards biomarkers and the implementation of a bio-sensitive grating into the array will be considered in future work.

Acknowledgments

This work was supported by the Engineering and Physical Sciences Research Council [grant numbers EP/N026985/1, EP/N025725/1]. The authors thank the Nanoscale and Microscale Research Centre (nmRC) for providing access to instrumentation.

References

[1] A.M. Norris, J.G. Hardman, T. Asai, A firm foundation for progress in airway management, Br. J. Anaesth. 106 (5) (2011) 613–616.
[2] The Presence and Sequence of Endotracheal Tube Colonization in Patients Undergoing Mechanical Ventilation, (2019).
[3] M.O. Al-Qadi, A.W. Artenstein, S.S. Braman, The 'forgotten zone': acquired disorders of the trachea in adults, Respir. Med. 107 (9) (2013) 1301–1313.
[4] T. Williams, Humidification in the intensive care unit, SAJCC 21 (26) (2005).
[5] J. Chastre, J.-Y. Fagon, Ventilator-associated pneumonia, Am. J. Respir. Crit. Care Med. 165 (no. 23) (2002) 867–903.
[6] F.U. Hernandez, R. Correia, S. Korposh, S.P. Morgan, B.R. Hayes-Gill, S.W. James, D. Evans, A. Norris, Measurements of endotracheal tube cuff contact pressure using fibre Bragg gratings, Proc. SPIE – Int. Soc. Opt. Eng. 9634 (2015).
[7] F. Chiavaioli, C.A.J. Gouveia, P.A.S. Jorge, F. Baldini, Towards a uniform metrological assessment of grating-based optical fiber sensors: from refractometers to biosensors, Biosensors 7 (2) (2017).
[8] A. Cusano, M. Consales, A. Crescitelli, M. Penza, P. Aversa, P.D. Veneri, M. Giordano, Charge transfer effects on the sensing properties of fiber optic chemical nano-sensors based on single-walled carbon nanotubes, Carbon N. Y. 47 (3) (2009) 782–788.
[9] Y. Kang, H. Ruan, Y. Wang, F.J. Arregui, I.R. Matias, R.O. Claus, Nanostructured optical fibre sensors for breathing airflow monitoring, Meas. Sci. Technol. 17 (5) (2006) 1207–1210.
[10] P.A. Janeesh, H. Sami, C.R. Dhanya, A. Abraham, RSC Advances Biocompatibility and genotoxicity studies of polyallylamine hydrochloride nanocapsules in rats, RSC Adv. (2014) 24484–24497.
[11] S. Murugadoss, D. Lison, L. Godderis, S. Van Den Brule, J. Mast, F. Brassinne, N. Sebaihi, P.H. Hoet, Toxicology of silica nanoparticles: an update, Arch. Toxicol. 91 (9) (2017) 2967–3010.
[12] S. Wagner, S. Munzer, P. Behrens, T. Scheper, Bahnemann Detlef, C. Kasper, Cytotoxicity of titanium and silicon dioxide nanoparticles cytotoxicity of titanium and silicon dioxide nanoparticles, J. Phys. Conf. Ser. 170 (2009).
[13] G. Rego, A review of refractometric sensors based on long period fibre gratings, Sci. World J. 2013 (2013).
[14] J. Hromadka, S. Korposh, M.C. Partridge, S.W. James, F. Davis, D. Crump, R.P. Tatam, Multi-parameter measurements using optical fibre long period gratings for indoor air quality monitoring, Sens. Actuators B Chem. 244 (2017) 217–225.
[15] R. Correia, S.W. James, S.P. Morgan, S.-W. Lee, S. Korposh, Biomedical application of optical fibre sensors, J. Opt. (2018).
[16] S.W. James, R.P. Tatam, Optical fibre long-period grating sensors: characteristics and application, Meas. Sci. Technol. 14 (5) (2003) R49–R61.
[17] H.J. Patrick, A.D. Kersey, F. Bucholtz, Analysis of the response of long period fiber gratings to external index of refraction, J. Lightwave Technol. 16 (9) (1998) 1606–1612.
[18] K. Ariga, Y. Yamauchi, G. Rydzek, Q. Ji, Y. Yonamine, K.C.-W. Wu, J.P. Hill, Layer-by-layer nanoarchitectonics: invention, innovation, and evolution, Chem. Lett. 43 (no. 1) (2014) 36–68.
[19] F.U. Hernandez, S.P. Morgan, B.R. Hayes-gill, D. Harvey, W. Kinnear, A. Norris, D. Evans, J.G. Hardman, S. Korposh, Characterization and use of a fiber optic sensor based on PAH/SiO_2 film for humidity sensing in ventilator care equipment, IEEE Trans. Biomed. Eng. 63 (9) (2016) 1985–1992.
[20] D. Gomez, S.P. Morgan, B.R. Hayes-Gill, R.G. Correia, S. Korposh, Polymeric optical fibre sensor coated by SiO_2 nanoparticles for humidity sensing in the skin microenvironment, Sens. Actuators B Chem. 254 (2018).
[21] Y. Luo, C. Chen, K. Xia, S. Peng, H. Guan, J. Tang, H. Lu, J. Yu, J. Zhang, Y. Xiao, Z. Chen, Tungsten disulfide (WS_2) based all-fiber-optic humidity sensor, Opt. Express 24 (8) (2016) p. 8956.
[22] Y. Xiao, J. Zhang, X. Cai, S. Tan, J. Yu, H. Lu, Y. Luo, G. Liao, S. Li, J. Tang, Z. Chen, Reduced graphene oxide for fiber-optic humidity sensing, Opt. Express 22 (25) (2014) p. 31555.
[23] R. Aneesh, S.K. Khijwania, Zinc oxide nanoparticle-doped nanoporous solgel fiber as a humidity sensor with enhanced sensitivity and large linear dynamic range, Appl. Opt. 52 (22) (2013) 5493–5499.
[24] J. Ascorbe, J. Corres, F. Arregui, I. Matias, Recent developments in fiber optics humidity sensors, Sensors 17 (4) (2017) p. 893.
[25] A. Urrutia, J. Goicoechea, A.L. Ricchiuti, D. Barrera, S. Sales, F.J. Arregui, Simultaneous measurement of humidity and temperature based on a partially coated optical fiber long period grating, Sens. Actuators B Chem. 227 (2016) 135–141.
[26] J. Hromadka, S. Korposh, M.C. Partridge, S.W. James, F. Davis, D. Crump, R.P. Tatam, Multi-parameter measurements using optical fibre long period gratings for indoor air quality monitoring, Sens. Actuators B Chem. 244 (2017).
[27] R.Y.N. Wong, E. Chehura, S.E. Staines, S.W. James, R.P. Tatam, Fabrication of fiber optic long period gratings operating at the phase matching turning point using an ultraviolet laser, Appl. Opt. 53 (21) (2014) 4669–4674.

[28] J. Hromadka, R. Correia, S. Korposh, Fabrication of fiber optic long period gratings operating at the phase matching turning point using an amplitude mask, Proc. SPIE – Int. Soc. Opt. Eng. 9916 (2016).
[29] C.S. Cheung, S.M. Topliss, S.W. James, R.P. Tatam, Response of fibre optic long period gratings operating near the phase matching turning point to the deposition of nanostructured coatings, J. Opt. Soc. Am. B 25 (6) (2008) 897–902.
[30] S. Korposh, S.W. James, S.-W. Lee, S. Topliss, S.C. Cheung, W.J. Batty, R.P. Tatam, Fiber optic long period grating sensors with a nanoassembled mesoporous film of SiO2 nanoparticles, Opt. Express. 18 (12) (2010) 13227–13238.
[31] S. Korposh, S.-W. Lee, S.W. James, R.P. Tatam, Refractive index sensitivity of fibre optic long period gratings with SiO_2 nanoparticle based mesoporous coatings, SPIE 7753 (2011) 19–22.
[32] D. Polito, M.A. Caponero, A. Polimadei, P. Saccomandi, C. Massaroni, S. Silvestri, E. Schena, A needle-like probe for temperature monitoring during laser ablation based on FBG: manufacturing and characterizatio, J. Med. Dev. 9 (c) (2015).
[33] S. Korposh, S.-W. Lee, S.W. James, R.P. Tatam, Refractive index sensitivity of fibre optic long period gratings with SiO2 nanoparticle based mesoporous coatings, Proc. SPIE – Int. Soc. Opt. Eng. 7753 (2011).
[34] Y. Chikata, M. Onodera, H. Imanaka, M. Nishimura, Temperature of gas delivered from ventilators, J. Intens. Care 1 (1) (2013) 2–5.